bioRxiv preprint doi: https://doi.org/10.1101/2020.12.01.407569; this version posted December 2, 2020. The copyright holder for this preprint (which was not certified by peer review) is the author/funder, who has granted bioRxiv a license to display the preprint in perpetuity. It is made available under aCC-BY-NC 4.0 International license.

Pan-genome analysis of *Mycobacterium tuberculosis* identifies accessory genome sequences deleted in modern Beijing lineage.

Running title: Mutations among drug resistant genes

Syed Beenish Rufai[1], Egon A. Ozer[2], Sarman Singh[3#]

[1]Division of Clinical Microbiology and Molecular Medicine, Department of Laboratory Medicine, All India Institute of Medical Sciences, New Delhi, India

[2]Department of Medicine, Division of Infectious Diseases, Nort h-western University Feinberg School of Medicine, Chicago, Illinois, USA

[3]Department of Microbiology All India Institute of Medical Sciences, Bhopal, India

 # Corresponding Author:

Prof. Sarman Singh, MD,

Department of Microbiology

All India Institute of Medical Sciences,

Saket Nagar, Bhopal (India)

Phone: +91-755-2672317, 2672111

Fax: +91-755-2672337

Email: sarman_singh@yahoo.com, sarman.singh@gmail.com

bioRxiv preprint doi: https://doi.org/10.1101/2020.12.01.407569; this version posted December 2, 2020. The copyright holder for this preprint (which was not certified by peer review) is the author/funder, who has granted bioRxiv a license to display the preprint in perpetuity. It is made available under aCC-BY-NC 4.0 International license.

Abstract (word count 235):

Beijing sub-lineage of *Mycobacterium tuberculosis* has been reported to have increased transmissibility and drug resistance. This led us to get insights of genomic landscape of modern Beijing sub-lineages in comparison with other lineages of *M. tuberculosis* utilizing pan-genomics approach. Pangenome analysis was performed using software Spine (v0.2.3), AGEnt (v0.2.3) and ClustAGE (v0.7.6). The average pangenome size was 45,40,849 bp with 4,391 coding sequences (CDS), with a GC content of 65.4%. The size of the core genome was 36,83,161 bp, contained 3,698 CDS and had an average GC content of 65.1%. The average accessory genome size was 6,96,320.9 bp, with 539.4 CDS and GC content of 67.9%. Among the accessory elements complete deletion of CRISPR-associated endoribonuclease cas1 (*Rv2817c*), cas2 (*Rv2816c*), CRISPR type III-a/mtube-associated protein csm6 (*Rv2818c*), CRISPR type III-a/mtube-associated ramp protein csm5 (*Rv2819c*) and partial deletion (61.5%) CRISPR type III-a/mtube-associated ramp protein csm4 (*Rv2820c*) sequences was found specifically in modern Beijing lineages taken in assortment. The sequences were validated using conventional PCR method, which precisely amplified the corresponding targets of sequence elements with 100% sensitivity and specificity. Deletion of accessory CRISPR sequence elements amongst the modern Beijing sub-lineage of *M. tuberculosis* suggest more defective DNA-repair in these strains which may enhance virulence of the strains. Further, the developed conventional PCR approach for detection of virulent modern Beijing lineage may be of interest to public health and outbreak control organizations for rapid detection of modern Beijing lineage.

bioRxiv preprint doi: https://doi.org/10.1101/2020.12.01.407569; this version posted December 2, 2020. The copyright holder for this preprint (which was not certified by peer review) is the author/funder, who has granted bioRxiv a license to display the preprint in perpetuity. It is made available under aCC-BY-NC 4.0 International license.

Introduction (3687):

The emergence of resistance towards first and second line anti-tuberculosis drugs in *M. tuberculosis* strains poses an increasing threat to public health (1). Estimates from TB investigation data predicts an expected increase in Multi-drug resistant (MDR) and extensively drug resistant (XDR) TB especially in developing countries like India, Philippines, Russia and South Africa (2). Classical techniques of determining genotyping and recently Whole genome sequencing (WGS) have revealed significant evolution of strains leading to diversity among human adapted *M. tuberculosis* strains, leading to acquire various genetic mechanisms for successful transmission and survival in the population (3)**.**

Among different lineage of lineages of *M. tuberculosis* which include lineages Indo Oceanic, Euro-American, Central Asian, and the East Asian (Beijing-sub lineage) is known to have originated out of East Asia and has disseminated around the world. The variability in gene expression patterns of different strains of *M. tuberculosis* during infection and intra/inter genomic variation among pathogenic strains has been documented as a significant feature in pathogenesis and types of infection caused by the strains (4). The Beijing sub-lineage is reported as more virulent in comparison to other lineages of *M. tuberculosis* in terms of an enhanced level of pathogenicity leading to increased transmissibility, rapid progression from latent to active disease, epidemiological association with transmission outbreaks and increased frequency of antibiotic resistance suggesting that genetic modifications distinguish the virulence and pathogenicity of this lineage (5–11). The global spread and association of Beijing strains with drug resistance has also been documented from India and other parts of world which is driving attention of researchers to further understand the genomic features that make this lineage more virulent in comparison to that of other lineages of *M. tuberculosis* (6, 8, 12–14).

bioRxiv preprint doi: https://doi.org/10.1101/2020.12.01.407569; this version posted December 2, 2020. The copyright holder for this preprint (which was not certified by peer review) is the author/funder, who has granted bioRxiv a license to display the preprint in perpetuity. It is made available under aCC-BY-NC 4.0 International license.

With the advent of next-generation sequencing (NGS) technologies, WGS has been used widely to identify evolutionary markers, polymorphism across lineages and mutations associated with drug resistance in *M. tuberculosis* (15). With availability of genomic databases and whole genome sequences of *M. tuberculosis*, approaches for deciphering novel mutations in comparison to reference strains are being utilized which results in loss of unique coding sequences(CDS)/genes that may have role in virulence or acquiring drug resistance (16).To overcome this, pan-genome based approach has been preferred which discern a more complete gene landscape for identification of unique (specific to single strains), accessory (shared among two or more strains) and core genes (present in all strains) for estimating the genomic diversity and identification of novel/unique gene sequences and discovery of markers for lineage identification (16–18).

WGS of *M. tuberculosis* isolates has been performed on isolates from Malaysia, China, Myanmar, Peru, Colombia, India, Ireland, New Zealand, Africa, Korea and Russia and large collection of genomes from clinical isolates of *M. tuberculosis* were analyzed by Manson et al 2017 [21–25]. But no pangenome studies were done on *M. tuberculosis* diversity of lineages to understand the variations in terms of unique genes/ sequences among them. This study was aimed to identify unique and shared sequences in the three laboratory sequenced TB isolates and WGS *M. tuberculosis* genomes data available in the public domain to decipher novel markers that may be questioned for higher virulence in the Beijing lineage.

Material and Methods:

This study was performed in an accredited TB laboratory in the Division of Clinical Microbiology & Molecular Medicine, All India Institute of Medical Sciences, New Delhi. Representative XDR-TB (L-823, L-182 and L-31) isolates of known drug susceptibility testing (DST) patterns and spoligotypes published previously were selected for WGS (19).

bioRxiv preprint doi: https://doi.org/10.1101/2020.12.01.407569; this version posted December 2, 2020. The copyright holder for this preprint (which was not certified by peer review) is the author/funder, who has granted bioRxiv a license to display the preprint in perpetuity. It is made available under aCC-BY-NC 4.0 International license.

Whole genome sequencing of three lab isolated XDR-TB:

Whole genome sequencing of the three XDR-TB isolates was performed using Ion Torrent PGM platform (Life Technologies). Briefly, DNA extraction was performed as previously described (20)**.** The three genomes were sequenced using Ion Torrent PGM as published previously (19). Sequencing data generated by Ion Torrent PGM was analyzed using the Torrent Suite Software. De-novo assembly of sequenced data was performed using ion-plugin-assembler St. Petersburg genome assembler (SPades) (v 3.1.0) (19, 21). The three whole genomes sequences were deposited in GenBank under the accession numbers NDYV00000000 for L-182 (beijing strain), NCTW00000000 for L-823 (beijing strain) and NDYU00000000 L-31 (central Asian strain).

Data mining of whole Genome Draft sequences of *M. tuberculosis* isolates from the NCBI genome database:

In order to understand complete genomic repertoire, analysis of different *M. tuberculosis* genomes was required for in depth analysis. Due to lack of funding we only did WGS of representative XDR-TB isolates. We explored the work of *Manson et al., 2017* which already have analyzed more than five thousand genomes different lineages and variable geographical diversity (Manson et al., 2017) and selected 91 genomes based on diversity of lineages and geographical locations (22). We performed random search in (https://www.ncbi.nlm.nih.gov/sra) using the search terms "*Mycobacterium tuberculosis*" and selected 25 genomes recently published from diverse geographical locations. A total 121 genomes were taken for pan-genome analysis as per the available computational feasibility in our setup. Among 121 draft genome assemblies, three were sequenced XDR-TB genomes at our setting, 116 were draft genome assemblies downloaded from NCBI and two were reference

bioRxiv preprint doi: https://doi.org/10.1101/2020.12.01.407569; this version posted December 2, 2020. The copyright holder for this preprint (which was not certified by peer review) is the author/funder, who has granted bioRxiv a license to display the preprint in perpetuity. It is made available under aCC-BY-NC 4.0 International license.

strains of *M. tuberculosis* under accession number NC_000962.3 and AL12345.6 respectively **(Supplementary Table 1)**.

Pan-genome analysis of 121 isolates:

Pan-genome analysis of isolates was performed using the software suite Spine, AGEnt and ClustAGE (17, 23). This software identifies the nucleotide sequences and associated annotations of the core, accessory and unique genome fractions of a sequenced strain population.

Spine v 0.2.3 was used for the identification of the conserved core genome sequence of the set of 121 *M. tuberculosis* genomes using H37Rv (NC_00926.3) as the reference genome sequence for a strict core genome (genomic sequence present in 100% of the strains) and using AL12345.6 as the reference genome for extraction of soft core genome (core genome sequence present in at least 90% of the strains) (17). AGEnt v0.2.3 was used for identifying accessory genomic elements (AGEs) in bacterial genomes by using an in-silico subtractive hybridization approach against a core genome generated using the Spine algorithm (17). ClustAGE (v0.7.5) was used to compare accessory genomic elements (AGEs) between genomes. The default threshold for alignments of 85% sequence identity over at least 100 bp was used (23).

Estimation of phylogenetic tree using kSNP 3.0:

kSNP3 program was used for construction of phylogenetic parsimony tree using pan-genome SNPs from a set of genome sequences without use of reference genome and parsimony tree that is estimated as a consensus of up to 100 equally parsimonious trees. Pan-genome parsimony tree was constructed using kSNP 3.0 (24). *K-chooser* was used to determine the optimum *k-mer* size, which was set at 21.

Visualization of trees:

bioRxiv preprint doi: https://doi.org/10.1101/2020.12.01.407569; this version posted December 2, 2020. The copyright holder for this preprint (which was not certified by peer review) is the author/funder, who has granted bioRxiv a license to display the preprint in perpetuity. It is made available under aCC-BY-NC 4.0 International license.

Trees were visualized using Interactive tree of Life (iTOL) V3 with Bootstrapped values of original and resampled tree https://itol.embl.de (25).

Functional annotation of core and accessory genomes sequences:

Functional annotation of core, accessory and unique genome sequences were transferred from orthologs of taxa group Actinobacteria (Mycobacteriacae) using EggnNOG mapper v2 (26). COG letter categories obtained were patterned for functional description in COG database (27).

Standardization of conventional PCR for validation of sequences on clinical isolates:

Primers were designed using Primer 3 (V 4.1.0) for validation of sequences/ genomic fractions specific to lineage found from pangenome data analysis (28). Designed primers were obtained from Eurofins, India. DNA was isolated from clinical isolates (50 Beijing strains and 50 non-Beijing strains) and subjected to PCR as follows: 2.5 µl of 10X buffer, 500 mM KCl] supplied with 1 ml of 50 mM MgCl2, 0·5 µl of stock 10mM dNTP, 20pmol of each primer and 1.25U of Taq DNA polymerase and 5µl of template DNA. Each PCR was started with a 'hot Start' for 2min at 95°C followed by denaturation (25 cycles each of 15 sec at 95°C), annealing (25 cycles each of 15 sec at 55°C) and extension (25 cycles each of 45 sec at 68°C), and a final extension for 1 cycle for 5 min at 68°C in a thermal Cycler (MJ Research, USA) and amplified products were resolved through 2% agarose gel in Tris-acetate buffer.

Results:

Description of *M. tuberculosis* data sets used in study:

Of total 121 genomes used in study, apart from two reference strains, 44 (36.3%) genomes were of African origin, 40 (31.4%) from Asia, 29 (23.1%) from Europe and 6 (4.9%) from

bioRxiv preprint doi: https://doi.org/10.1101/2020.12.01.407569; this version posted December 2, 2020. The copyright holder for this preprint (which was not certified by peer review) is the author/funder, who has granted bioRxiv a license to display the preprint in perpetuity. It is made available under aCC-BY-NC 4.0 International license.

America. Place of origin and accession numbers of all draft genomes are mentioned in **(Supplementary Table 1)**.

Genome assembly statistics of three XDR-TB isolates:

De novo sequence assembly was performed using SPAdes v3.1.0 and functional annotation performed using RAST (Rapid Annotation using Subsystem Technology) yielding total genome sizes of 4,201,682, 4,288,294 and 4,311,779 bp with 65, 65.4 and 65.3% GC contents, and coding sequences of 4516, 4737 and 4813 for L-823, L-182 and L-31 respectively(19). Using spoligotyping technique, L-182 and L-823 were found to be Beijing sub-lineage of ST1 and ST236, and L-31 was found to be central Asian strain of ST1120 as per the SITVIT2 database (29).

Construction of parsimony and core genome tree:

Unrooted phylogenetic tree was constructed comparing the 121 WGS genome sequences in the context of the *M. tuberculosis* lineages circulating globally **(Figure 1)**. Total of 18,025 variable single nucleotide positions were extracted from these genome sequences to construct a phylogenetic parsimony tree. Among the genomes with known lineages, three genomes from each lineage group were taken as reference. After analysis, *M. tuberculosis* genomes were dispersed among four lineages Lineage 1(8; 6.6%), Lineage 2 (42; 34.7%), Lineage 3 (8; 6.6%) and Lineage 4 (63; 52.1%) respectively **(Supplementary Table 2)**.

Description of pan-genome (hard core, soft core and accessory genome):

Total pan-genome size was estimated to be 4,540,489 bp with 4391 coding sequences (CDS), and a GC content of 65.4%. Estimated average size of the hard-core genome (i.e., sequence present in 100% of genomes) was 3,683,161 bp (81.1% of total genome size), contained 3,698 coding sequences (CDS) and had an average GC content of 65.1% as compared to the average

bioRxiv preprint doi: https://doi.org/10.1101/2020.12.01.407569; this version posted December 2, 2020. The copyright holder for this preprint (which was not certified by peer review) is the author/funder, who has granted bioRxiv a license to display the preprint in perpetuity. It is made available under aCC-BY-NC 4.0 International license.

188 accessory genome size of 696,320.9 bp (15.3%), and GC content of 67.9%. Estimated average
189 size of the soft-core genome (i.e. sequence present in ≥ 90% genomes) was 4,308,602 bp
190 (94.8% of total genome size), contained 4,237 CDS and had an average GC content of 65.4%
191 as compared to the average accessory genome size 93,819.7 bp (2.1%), with 57.6 CDS and GC
192 content of 71.7% **(Table 1) (Supplementary Table 3)**.

193 **Determination of core genome:**

194 In order to better estimate the likely species core genome size, a rigorous definition of core
195 genome was used. Core genome represented a total of 81.1% of the overall pan-genome
196 repertoire. The average amount of core genome and pan-genome as a function of the number
197 of reference genome (NC_000962.3) included in the analysis was computed using an
198 adaptation of the method described by *Tettelin et al 2005* (16) **(Fig 2 & 3).**

199 **Functional annotation of core and accessory genome elements:**

200 Functional annotation of coding sequences (CDS) associated with hard-core and accessory
201 genome were analyzed using EggNOG mapper v2. Coding sequences belonging to the core
202 genomes were assigned to putative super-functional **(Fig 4A)** and functional **(Fig 4B)**
203 categories using the Clusters of Orthologous Groups of proteins (COG) database. Matching of
204 gene ontology terms with COG database predicted more than half of CDS in core genome were
205 dedicated with metabolism functions, one fourth was of unknown function or poorly
206 characterized and rest of CDS were involved in cellular processes and signaling, and
207 Information storage and processing.

208 Coding sequences belonging to the accessory genomes were assigned to putative super-
209 functional **(Fig 4A)** and functional **(Figure 4B)** categories using COG database which
210 predicted one fourth of CDS in accessory genome were dedicated with metabolism, nearly one

bioRxiv preprint doi: https://doi.org/10.1101/2020.12.01.407569; this version posted December 2, 2020. The copyright holder for this preprint (which was not certified by peer review) is the author/funder, who has granted bioRxiv a license to display the preprint in perpetuity. It is made available under aCC-BY-NC 4.0 International license.

fourth of all CDS were associated with cellular and signaling processes, and Information storage and processing. Rest of the CDS were of unknown function.

Functional annotation of CDS associated with unique accessory elements (unique to each genome) predicted most of the genes that were acquired during the adaptation were associated with metabolism (26%), cell storage and signaling (25%), information storage and processing (20%) and rest of CDS were associated with unknown function or poorly characterized **(Fig 5)**. Variation of accessory genomic elements, among soft- and hard-core components are shown in heat map generated by ClustAGE software **(Fig. 6)**.

Clustering, distribution analysis and functional annotation of accessory nucleotide sequences:

Accessory genomic elements (AGE's) in the population, also referred to as bins, were identified using ClustAGE software (23). A total of 651 individual AGE's hereafter referred as bins were found to be present in total input of 121 genomes that ranged in size from 201 bp to 37765 bp. The average size of the bins (651bins) was 1230.5 bp. These bins were further subdivided to sub-elements in order to see sharing and unique sequence elements among genomes. Total 859 sub-elements of sizes more than 200 bp were found in these genomes (n > 1). Shared sequences obtained from accessory elements obtained on analysing hard-core repertoire in *M. tuberculosis* strains (90%) as shown in ClustAGE plots (**Fig 7A** & **7B)**. Of the total genomes taken in assortment, 11 (9%) of *M. tuberculosis* genomes was having 139 unique sub-elements with an average length of 459.6 bp.

Identification of novel markers among AGE's:

Among the shared accessory genome sequences, portions of one 4487 bp AGE (bin 32) was found to be absent in all of the Beijing genomes **(Fig 8)**. To better understand the nature of the deleted genomic sequence, bin 32 was further divided into discrete sub elements which

bioRxiv preprint doi: https://doi.org/10.1101/2020.12.01.407569; this version posted December 2, 2020. The copyright holder for this preprint (which was not certified by peer review) is the author/funder, who has granted bioRxiv a license to display the preprint in perpetuity. It is made available under aCC-BY-NC 4.0 International license.

revealed the portion of the AGE missing in the Beijing lineage strains, named bin32se-0001, encoded all or some of the following genes: CRISPR-associated endo-ribonuclease cas2 (100%); CRISPR-associated endonuclease cas1 (100%); CRISPR type III-a/mtube-associated protein csm6 (100%); CRISPR type III-a/mtube-associated protein csm5 (100%;) and CRISPR type III-a/mtube-associated ramp protein csm4 (61.5%) **(Table 2).**

Standardization of PCR for validation of sequences on clinical isolates:

Designed primers were used for convention PCR for validation of sequences on culture isolates. Designed primers specific for CRISPR sequences are mentioned in **(Table 3)**. The PCR precisely amplified the corresponding targets from DNA isolated from the 50 non-Beijing strains and control strain H37Rv. No amplification was seen among the 50 DNA samples isolated from Beijing isolates **(Fig 9A, 9B)**. Spoligotyping patterns of isolates used for evaluation are mentioned in **(Table 4).**

Discussion :

The main causative agent of TB in humans *M. tuberculosis sensu stricto* and of major concern is uncontrolled spread of drug resistance in developing countries (30). Total of four lineages (lineage 1-4) have been recognized within the *M. tuberculosis* species showing difference in characteristics in terms of evolutionary position, transmissibility, drug resistance, host interaction, latency, and vaccine efficacy (31). With growing evidence, it is known that genetic diversity of *M. tuberculosis* may have significant clinical consequences and sub-lineages were also reported to show similar variation characteristics especially Beijing sub-lineage (East Asian, Lineage 2). During evolution, this strain have been proposed to possess selective advantages, in contrast to other *M. tuberculois* lineages, which resulted in drug resistant TB outbreaks, increasing in population size especially in settings with distinct levels of TB incidence levels, rapid progression of disease after infection and unfavorable treatment

bioRxiv preprint doi: https://doi.org/10.1101/2020.12.01.407569; this version posted December 2, 2020. The copyright holder for this preprint (which was not certified by peer review) is the author/funder, who has granted bioRxiv a license to display the preprint in perpetuity. It is made available under aCC-BY-NC 4.0 International license.

outcome (7, 18, 19, 30–33). These findings make it crucial to understand what deviations had been altered in genome of Beijing lineage during the evolution in comparison to other lineages, resulting in excessive virulence of the strain.

To gain insights, studies have been performed to find evolutionary markers specific to Lineage2 which resulted in identification of polymorphism in noise transfer function region (NTF) locus, mutT2 and mutT4 genes, in some strains named as modern beijing sub-lineages which were predicted to be more virulent than ancient or prototype Beijing lineages (6, 34–36). Moreover, other markers like mutation in hspX gene, deletion of *Rv0279c* in some beijing isolates gene and RD207 in all beijing isolates (*Rv2815c-Rv2820c*) were also interpreted (37, 38). As, SNPs are consistent and phylogenetically useful markers, since the low sequence distinction and lack of horizontal gene transfer in *M. tuberculosis* make independent recurrent mutations unlikely (39). We thus used comparative genomics approach to provides insight into features of shared/ unique coding sequences across different lineages of *M. tuberculosis* (23).

As expected, the predicted core genome size of *M. tuberculosis* genome repertoire was 81% of total pan-genome size for hard core genome and 95% for soft core genome representing highly conserved nature of this bacterium. In order to determine extra genes that are added in each newly sequenced genome of *M. tuberculosis* we used the concept of open/closed pan-genome (40). We predicted *M. tuberculosis* genome taken in assortment as an “open” pan-genome (as the average number of genes with each new genome shows no sign of plateauing) which specify that each new genome sequenced will provide new/novel genes, and overall increase the size of pan-genome (16). These findings correlate with previous pan-genome finding performed on Mycobacterium species (41, 42) [39]. Although, this approach of determining “open” pan-genome is mathematical extrapolation from the available sequenced genomes, however, it supports the fact that some species have tremendously flexible genetic content (40). This open/finite pan-genome implies the number of distinct genes found in *M. tuberculosis* strains

bioRxiv preprint doi: https://doi.org/10.1101/2020.12.01.407569; this version posted December 2, 2020. The copyright holder for this preprint (which was not certified by peer review) is the author/funder, who has granted bioRxiv a license to display the preprint in perpetuity. It is made available under aCC-BY-NC 4.0 International license.

is infinite as opposed to finite number of genes in a closed and thus increased emerging rate of drug resistance **(Fig 2 & Fig 3)** (41).

We found a major proportion of estimated CDS (in hard core genome) dedicated to metabolism [which consists of sequences mostly related with energy production and conversion (C), Amino acid transport and metabolism (E) and Lipid transport and metabolism (I)] **(Fig 4A & Fig 4B)**. This shows, that these sets of CDS in *M. tuberculosis* are conserved under selective pressure during its long-term interactions with its human host. The CDS associated with metabolic function may have major role in mycobacterial persistence, host pathogen struggle for nutrients, immune recognition and can be target for drug discovery [41] **(Warner, 2015)**. Average accessory genome sequences covered almost 15% of total genome repertoire, and functions of the CDS were mainly dedicated to category of poorly characterized or unknown function (S) followed by metabolism [coenzyme transport & metabolism (H)], and cellular processes &signaling [cell wall membrane envelope (M)] **(Fig 4A & Fig 4B)**. Among the poorly characterized CDS were mainly hypothetical proteins, PPE family protein, PE-PGRS family protein, PE family protein and mobile genetic elements. *M. tuberculosis* genomes containing PE/PPE family proteins have been reported as polymorphic having role in bacterial virulence and advances have been used towards the expansion of these family proteins for vaccine development (43). With such strain diversity as observed in our genome assortment taken in our study among PE/PPE family proteins there are chances for negative vaccine effectiveness however, more studies are required to prove the statement (44) (McEvoy et al., 2012).The accessory genome sequences may result in providing emergence of new functions, strain variations and understanding how it manages to survive in different niches, drug pressure which can give a reflection of its life style characteristic associated with virulence or resistance to antibiotics, it may be adapting during the course of evolution.

bioRxiv preprint doi: https://doi.org/10.1101/2020.12.01.407569; this version posted December 2, 2020. The copyright holder for this preprint (which was not certified by peer review) is the author/funder, who has granted bioRxiv a license to display the preprint in perpetuity. It is made available under aCC-BY-NC 4.0 International license.

Unique genomic fractions were also observed in *M. tuberculosis* genomes, and were related to amino acid transport and metabolism (E), followed by Replication, recombination and repair (L) and Translation, ribosomal structure and biogenesis (J). These findings also provide information for the uptake of unique/novel genes in order to compensate the cost fitness due to antibiotic pressure. We observed majority of drug resistant *M. tuberculosis* genes were found in predicted hard-core genome except pncA (115/121 isolates). Thus, pncA gene mutations may have lower sensitivity in detection in 100% of *M. tuberculosis* strains and can be detected in a clear mainstream (>90%) of PZA-resistant strains, which has also been reported previously (45).

Our main findings during the pan-genome analysis in our collection of 121 *M. tuberculosis* genomes, we found CDS absent in modern Beijing lineage viz; CRISPR-associated endoribonuclease cas2 (100%); CRISPR-associated endonuclease cas1 (100%); CRISPR type III-a/mtube-associated protein csm6 (100%) and CRISPR type III-a/mtube-associated ramp protein csm4 (61.5%) respectively. However, we didn't find these deletions in two genomes of Lineage 2, these two strains have been reported as prototype Beijing like harboring an ancestral- spoligotype, which is close to the Beijing clade of East Asia lineage with Spoldb4 international data base code as 246 and 643 (46). CRISPR-Cas system in *M. tuberculosis* associated with Cas1 and Cas2 genes perform endogenous DNA-repair along with a Type III A (CSM) effector arrangement, providing adaptive immunity to bacteriophages and plasmids. Deletion of the CRISPR-Cas system with associated Cas1 and Cas2 genes along with Type III A (CSM) among Beijing lineage strains could suggest more defective DNA-repair genes in such strains resulting in additional variability (47). This could predispose the lineage to development of drug resistance and transmission in the community. Such sequence markers could be useful in geographical regions where predominance of Beijing lineage is suspected. Beijing lineage that is vulnerable to first- and second-line TB drugs and has role in MDR-TB

bioRxiv preprint doi: https://doi.org/10.1101/2020.12.01.407569; this version posted December 2, 2020. The copyright holder for this preprint (which was not certified by peer review) is the author/funder, who has granted bioRxiv a license to display the preprint in perpetuity. It is made available under aCC-BY-NC 4.0 International license.

transmission. We also validated the CRISPR sequences that we predicted to be deleted in modern beijing lineages on lab isolates having different spoligotype patterns **(Table 4)** using conventional PCR method, which resulted in 100% sensitivity and specificity. This will facilitate molecular epidemiological studies and may contribute in the identification of virulent Beijing strains. Additional evidences including expression of cas1 and cas2 gene across *M. tuberculosis* lineages need to be verified to conclude that deletion of these genes lead to increased sensitivity to DNA damage resulting it in a potential phenotype mutator.

Conclusion: We conclude *M. tuberculosis* with an open pan-genome, presence of unique genome sequence fractions which may have significant role to persist in host, tolerating antibiotic pressure and developing drug resistance. Moreover, we found modern Beijing strains to have accessory sequences elements deleted which may have role in virulence and adaptation among these strains. Further, in-depth gene expression studies are required to understand the role of such sequences in Beijing Lineage.

Acknowledgement:

A fellowship to S.B.R. from the All India Institute of Medical Sciences, New Delhi, India (reference number P-2012/12452) is likewise acknowledged. This study was supported by a grant from the Department of Biotechnology of the Government of India (BT/538/NE/TBP/2013) and the Indian Council of Medical Research (5/8/5/41/2016/ECD-I).

bioRxiv preprint doi: https://doi.org/10.1101/2020.12.01.407569; this version posted December 2, 2020. The copyright holder for this preprint (which was not certified by peer review) is the author/funder, who has granted bioRxiv a license to display the preprint in perpetuity. It is made available under aCC-BY-NC 4.0 International license.

355 **References:**

356 1. Lange C, Chesov D, Heyckendorf J, Leung CC, Udwadia Z, Dheda K. 2018. Drug-
357 resistant tuberculosis: An update on disease burden, diagnosis and treatment.
358 Respirology 23:656–673.

359 2. Sharma A, Hill A, Kurbatova E, van der Walt M, Kvasnovsky C, Tupasi TE, Caoili JC,
360 Gler MT, Volchenkov GV, Kazennyy BY, Demikhova OV, Bayona J, Contreras C,
361 Yagui M, Leimane V, Cho SN, Kim HJ, Kliiman K, Akksilp S, Jou R, Ershova J,
362 Dalton T, Cegielski P, Global Preserving Effective TB Treatment Study Investigators.
363 2017. Estimating the future burden of multidrug-resistant and extensively drug-resistant
364 tuberculosis in India, the Philippines, Russia, and South Africa: a mathematical
365 modelling study. The Lancet Infectious Diseases 17:707–715.

366 3. Murase Y, Maeda S, Yamada H, Ohkado A, Chikamatsu K, Mizuno K, Kato S, Mitarai
367 S. 2010. Clonal Expansion of Multidrug-Resistant and Extensively Drug-Resistant
368 Tuberculosis, Japan. Emerg Infect Dis 16:948–954.

369 4. Jena L, Kashikar S, Kumar S, Harinath BC. 2013. Comparative proteomic analysis of
370 Mycobacterium tuberculosis strain H37Rv versus H37Ra. International Journal of
371 Mycobacteriology 2:220–226.

372 5. Ford CB, Shah RR, Maeda MK, Gagneux S, Murray MB, Cohen T, Johnston JC, Gardy
373 J, Lipsitch M, Fortune SM. 2013. Mycobacterium tuberculosis mutation rate estimates
374 from different lineages predict substantial differences in the emergence of drug resistant
375 tuberculosis. Nat Genet 45:784–790.

bioRxiv preprint doi: https://doi.org/10.1101/2020.12.01.407569; this version posted December 2, 2020. The copyright holder for this preprint (which was not certified by peer review) is the author/funder, who has granted bioRxiv a license to display the preprint in perpetuity. It is made available under aCC-BY-NC 4.0 International license.

376 6. Mokrousov I, Narvskaya O, Otten T, Vyazovaya A, Limeschenko E, Steklova L,
377 Vyshnevskyi B. 2002. Phylogenetic reconstruction within Mycobacterium tuberculosis
378 Beijing genotype in northwestern Russia. Research in Microbiology 153:629–637.

379 7. Thwaites G, Caws M, Chau TTH, D'Sa A, Lan NTN, Huyen MNT, Gagneux S, Anh
380 PTH, Tho DQ, Torok E, Nhu NTQ, Duyen NTH, Duy PM, Richenberg J, Simmons C,
381 Hien TT, Farrar J. 2008. Relationship between Mycobacterium tuberculosis Genotype
382 and the Clinical Phenotype of Pulmonary and Meningeal Tuberculosis. Journal of
383 Clinical Microbiology 46:1363–1368.

384 8. Glynn JR, Whiteley J, Bifani PJ, Kremer K, van Soolingen D. 2002. Worldwide
385 Occurrence of Beijing/W Strains of Mycobacterium tuberculosis: A Systematic Review.
386 Emerg Infect Dis 8:843–849.

387 9. Toungoussova OS, Caugant DA, Sandven P, Mariandyshev AO, Bjune G. 2004. Impact
388 of drug resistance on fitness of Mycobacterium tuberculosis strains of the W-Beijing
389 genotype. FEMS immunology and medical microbiology 42:281–290.

390 10. Anh DD, Borgdorff MW, Van LN, Lan NTN, Gorkom T van, Kremer K, Soolingen D
391 van. Mycobacterium tuberculosis Beijing Genotype Emerging in Vietnam - Volume 6,
392 Number 3—June 2000 - Emerging Infectious Diseases journal - CDC
393 https://doi.org/10.3201/eid0603.000312.

394 11. Iwamoto T, Yoshida S, Suzuki K, Wada T. 2008. Population structure analysis of the
395 Mycobacterium tuberculosis Beijing family indicates an association between certain
396 sublineages and multidrug resistance. Antimicrobial Agents and Chemotherapy
397 52:3805–3809.

bioRxiv preprint doi: https://doi.org/10.1101/2020.12.01.407569; this version posted December 2, 2020. The copyright holder for this preprint (which was not certified by peer review) is the author/funder, who has granted bioRxiv a license to display the preprint in perpetuity. It is made available under aCC-BY-NC 4.0 International license.

12. Baranov AA, Mariandyshev AO, Mannsåker T, Dahle UR, Bjune GA. 2009. Molecular epidemiology and drug resistance of widespread genotypes of Mycobacterium tuberculosis in northwestern Russia. The International Journal of Tuberculosis and Lung Disease: The Official Journal of the International Union Against Tuberculosis and Lung Disease 13:1288–1293.

13. Buu TN, Huyen MN, Lan NTN, Quy HT, Hen NV, Zignol M, Borgdorff MW, Cobelens FGJ, van Soolingen D. 2009. The Beijing genotype is associated with young age and multidrug-resistant tuberculosis in rural Vietnam. The International Journal of Tuberculosis and Lung Disease: The Official Journal of the International Union Against Tuberculosis and Lung Disease 13:900–906.

14. Rufai SB, Singh J, Kumar P, Mathur P, Singh S. 2018. Association of gyrA and rrs gene mutations detected by MTBDR sl V1 on Mycobacterium tuberculosis strains of diverse genetic background from India. 1. Scientific Reports 8:9295.

15. Iketleng T, Lessells R, Dlamini MT, Mogashoa T, Mupfumi L, Moyo S, Gaseitsiwe S, de Oliveira T. 2018. Mycobacterium tuberculosis Next-Generation Whole Genome Sequencing: Opportunities and Challenges. Tuberc Res Treat 2018.

16. Medini D, Donati C, Tettelin H, Masignani V, Rappuoli R. 2005. The microbial pan-genome. Curr Opin Genet Dev 15:589–594.

17. Ozer EA, Allen JP, Hauser AR. 2014. Characterization of the core and accessory genomes of Pseudomonas aeruginosa using bioinformatic tools Spine and AGEnt. BMC Genomics 15:737.

18. Liu W, Zou D, He X, Ao D, Su Y, Yang Z, Huang S, Zhao Q, Tang Y, Ma W, Lu Y, Wang J, Wang X, Huang L. 2018. Development and application of a rapid

bioRxiv preprint doi: https://doi.org/10.1101/2020.12.01.407569; this version posted December 2, 2020. The copyright holder for this preprint (which was not certified by peer review) is the author/funder, who has granted bioRxiv a license to display the preprint in perpetuity. It is made available under aCC-BY-NC 4.0 International license.

421 Mycobacterium tuberculosis detection technique using polymerase spiral reaction. 1.
422 Scientific Reports 8:3003.

423 19. Rufai SB, Singh S. 2019. Whole-Genome Sequencing of Two Extensively Drug-
424 Resistant Mycobacterium tuberculosis Isolates from India. Microbiol Resour Announc
425 8.

426 20. 1990. Molecular cloning: A laboratory manual. Second edition. Volumes 1, 2, and 3.
427 Current protocols in molecular biology. Volumes 1 and 2: By J. Sambrook, E. F.
428 Fritsch, and T. Maniatis. Cold Spring Harbor, New York: Cold Spring Harbor
429 Laboratory Press. (1989). 1626 pp. $115.00. Edited by F. M. Ausubel, R. Brent, R. E.
430 Kingston, D. D. Moore, J. G. Seidman, J. A. Smith, and K. Struhl. New York: Greene
431 Publishing Associates and John Wiley & Sons. (1989). 1120 pp. $255.00. Cell 61:17–
432 18.

433 21. Homer N, Merriman B, Nelson SF. 2009. BFAST: an alignment tool for large scale
434 genome resequencing. PLoS One 4:e7767.

435 22. Manson AL, Cohen KA, Abeel T, Desjardins CA, Armstrong DT, Barry CE, Brand J,
436 TBResist Global Genome Consortium, Chapman SB, Cho S-N, Gabrielian A, Gomez J,
437 Jodals AM, Joloba M, Jureen P, Lee JS, Malinga L, Maiga M, Nordenberg D, Noroc E,
438 Romancenco E, Salazar A, Ssengooba W, Velayati AA, Winglee K, Zalutskaya A, Via
439 LE, Cassell GH, Dorman SE, Ellner J, Farnia P, Galagan JE, Rosenthal A, Crudu V,
440 Homorodean D, Hsueh P-R, Narayanan S, Pym AS, Skrahina A, Swaminathan S, Van
441 der Walt M, Alland D, Bishai WR, Cohen T, Hoffner S, Birren BW, Earl AM. 2017.
442 Genomic analysis of globally diverse Mycobacterium tuberculosis strains provides
443 insights into the emergence and spread of multidrug resistance. Nat Genet 49:395–402.

bioRxiv preprint doi: https://doi.org/10.1101/2020.12.01.407569; this version posted December 2, 2020. The copyright holder for this preprint (which was not certified by peer review) is the author/funder, who has granted bioRxiv a license to display the preprint in perpetuity. It is made available under aCC-BY-NC 4.0 International license.

444 23. Ea O. 2018. ClustAGE: a tool for clustering and distribution analysis of bacterial
445 accessory genomic elements. BMC Bioinformatics 19:150–150.

446 24. kSNP3.0: SNP detection and phylogenetic analysis of genomes without genome
447 alignment or reference genome | Bioinformatics | Oxford Academic.

448 25. Letunic I, Bork P. 2019. Interactive Tree Of Life (iTOL) v4: recent updates and new
449 developments. Nucleic Acids Res 47:W256–W259.

450 26. Huerta-Cepas J, Szklarczyk D, Forslund K, Cook H, Heller D, Walter MC, Rattei T,
451 Mende DR, Sunagawa S, Kuhn M, Jensen LJ, von Mering C, Bork P. 2016. eggNOG
452 4.5: a hierarchical orthology framework with improved functional annotations for
453 eukaryotic, prokaryotic and viral sequences. Nucleic Acids Res 44:D286-293.

454 27. Tatusov RL, Natale DA, Garkavtsev IV, Tatusova TA, Shankavaram UT, Rao BS,
455 Kiryutin B, Galperin MY, Fedorova ND, Koonin EV. 2001. The COG database: new
456 developments in phylogenetic classification of proteins from complete genomes.
457 Nucleic Acids Res 29:22–28.

458 28. Untergasser A, Cutcutache I, Koressaar T, Ye J, Faircloth BC, Remm M, Rozen SG.
459 2012. Primer3—new capabilities and interfaces. Nucleic Acids Research 40:e115–e115.

460 29. Demay C, Liens B, Burguière T, Hill V, Couvin D, Millet J, Mokrousov I, Sola C,
461 Zozio T, Rastogi N. 2012. SITVITWEB – A publicly available international
462 multimarker database for studying Mycobacterium tuberculosis genetic diversity and
463 molecular epidemiology. Infection, Genetics and Evolution 12:755–766.

464 30. Merker M, Blin C, Mona S, Duforet-Frebourg N, Lecher S, Willery E, Blum MGB,
465 Rüsch-Gerdes S, Mokrousov I, Aleksic E, Allix-Béguec C, Antierens A,

bioRxiv preprint doi: https://doi.org/10.1101/2020.12.01.407569; this version posted December 2, 2020. The copyright holder for this preprint (which was not certified by peer review) is the author/funder, who has granted bioRxiv a license to display the preprint in perpetuity. It is made available under aCC-BY-NC 4.0 International license.

466 Augustynowicz-Kopeć E, Ballif M, Barletta F, Beck HP, Barry CE, Bonnet M, Borroni
467 E, Campos-Herrero I, Cirillo D, Cox H, Crowe S, Crudu V, Diel R, Drobniewski F,
468 Fauville-Dufaux M, Gagneux S, Ghebremichael S, Hanekom M, Hoffner S, Jiao W,
469 Kalon S, Kohl TA, Kontsevaya I, Lillebæk T, Maeda S, Nikolayevskyy V, Rasmussen
470 M, Rastogi N, Samper S, Sanchez-Padilla E, Savic B, Shamputa IC, Shen A, Sng L-H,
471 Stakenas P, Toit K, Varaine F, Vukovic D, Wahl C, Warren R, Supply P, Niemann S,
472 Wirth T. 2015. Evolutionary history and global spread of the Mycobacterium
473 tuberculosis Beijing lineage. 3. Nature Genetics 47:242–249.

474 31. Senghore M, Diarra B, Gehre F, Otu J, Worwui A, Muhammad AK, Kwambana-Adams
475 B, Kay GL, Sanogo M, Baya B, Orsega S, Doumbia S, Diallo S, de Jong BC, Pallen MJ,
476 Antonio M. 2020. Evolution of Mycobacterium tuberculosis complex lineages and their
477 role in an emerging threat of multidrug resistant tuberculosis in Bamako, Mali. Sci Rep
478 10.

479 32. Hang NTL, Maeda S, Keicho N, Thuong PH, Endo H. 2015. Sublineages of
480 Mycobacterium tuberculosis Beijing genotype strains and unfavorable outcomes of anti-
481 tuberculosis treatment. Tuberculosis 95:336–342.

482 33. Gagneux S, Small PM. 2007. Global phylogeography of Mycobacterium tuberculosis
483 and implications for tuberculosis product development. The Lancet Infectious Diseases
484 7:328–337.

485 34. Ebrahimi-Rad M, Bifani P, Martin C, Kremer K, Samper S, Rauzier J, Kreiswirth B,
486 Blazquez J, Jouan M, van Soolingen D, Gicquel B. 2003. Mutations in putative mutator
487 genes of Mycobacterium tuberculosis strains of the W-Beijing family. Emerging
488 Infectious Diseases 9:838–845.

bioRxiv preprint doi: https://doi.org/10.1101/2020.12.01.407569; this version posted December 2, 2020. The copyright holder for this preprint (which was not certified by peer review) is the author/funder, who has granted bioRxiv a license to display the preprint in perpetuity. It is made available under aCC-BY-NC 4.0 International license.

489 35. Marcos LA, Spitzer ED, Mahapatra R, Ma Y, Halse TA, Shea J, Isabelle M, Lapierre P,
490 Escuyer VE. Mycobacterium orygis Lymphadenitis in New York, USA - Volume 23,
491 Number 10—October 2017 - Emerging Infectious Diseases journal - CDC
492 https://doi.org/10.3201/eid2310.170490.

493 36. Rindi L, Lari N, Cuccu B, Garzelli C. 2009. Evolutionary pathway of the Beijing
494 lineage of Mycobacterium tuberculosis based on genomic deletions and mutT genes
495 polymorphisms. Infect Genet Evol 9:48–53.

496 37. Seyed Majidi A, Bazzazi H, Zamani S, Ghaemi EA. 2020. Comparison of hspX gene
497 sequence in the Beijing and non-Beijing Mycobacterium tuberculosis. Journal of
498 Clinical Tuberculosis and Other Mycobacterial Diseases 21:100187.

499 38. Stavrum R, Valvatne H, Bø TH, Jonassen I, Hinds J, Butcher PD, Grewal HMS. 2008.
500 Genomic Diversity among Beijing and non-Beijing Mycobacterium tuberculosis
501 Isolates from Myanmar. PLOS ONE 3:e1973.

502 39. Jones RC, Harris LG, Morgan S, Ruddy MC, Perry M, Williams R, Humphrey T,
503 Temple M, Davies AP. 2019. Phylogenetic Analysis of Mycobacterium tuberculosis
504 Strains in Wales by Use of Core Genome Multilocus Sequence Typing To Analyze
505 Whole-Genome Sequencing Data. Journal of Clinical Microbiology 57.

506 40. Guimarães LC, Florczak-Wyspianska J, de Jesus LB, Viana MVC, Silva A, Ramos RTJ,
507 Soares S de C, Soares S de C. 2015. Inside the Pan-genome - Methods and Software
508 Overview. Curr Genomics 16:245–252.

509 41. Periwal V, Patowary A, Vellarikkal SK, Gupta A, Singh M, Mittal A, Jeyapaul S,
510 Chauhan RK, Singh AV, Singh PK, Garg P, Katoch VM, Katoch K, Chauhan DS,
511 Sivasubbu S, Scaria V. 2015. Comparative Whole-Genome Analysis of Clinical Isolates

bioRxiv preprint doi: https://doi.org/10.1101/2020.12.01.407569; this version posted December 2, 2020. The copyright holder for this preprint (which was not certified by peer review) is the author/funder, who has granted bioRxiv a license to display the preprint in perpetuity. It is made available under aCC-BY-NC 4.0 International license.

512 Reveals Characteristic Architecture of Mycobacterium tuberculosis Pangenome. PLoS
513 One 10.

514 42. Yang T, Zhong J, Zhang J, Li C, Yu X, Xiao J, Jia X, Ding N, Ma G, Wang G, Yue L,
515 Liang Q, Sheng Y, Sun Y, Huang H, Chen F. 2018. Pan-Genomic Study of
516 Mycobacterium tuberculosis Reflecting the Primary/Secondary Genes,
517 Generality/Individuality, and the Interconversion Through Copy Number Variations.
518 Front Microbiol 9.

519 43. Campuzano J, Aguilar D, Arriaga K, León JC, Salas-Rangel LP, González-y-Merchand
520 J, Hernández-Pando R, Espitia C. 2007. The PGRS domain of Mycobacterium
521 tuberculosis: PE_PGRS Rv1759c antigen is an efficient subunit vaccine to prevent
522 reactivation in a murine model of chronic tuberculosis. Vaccine 25:3722–3729.

523 44. McEvoy CRE, Cloete R, Müller B, Schürch AC, van Helden PD, Gagneux S, Warren
524 RM, Gey van Pittius NC. 2012. Comparative analysis of Mycobacterium tuberculosis pe
525 and ppe genes reveals high sequence variation and an apparent absence of selective
526 constraints. PLoS One 7:e30593.

527 45. Werngren J, Alm E, Mansjö M. 2017. Non-pncA Gene-Mutated but Pyrazinamide-
528 Resistant Mycobacterium tuberculosis: Why Is That? Journal of Clinical Microbiology
529 55:1920–1927.

530 46. Kuan CS, Chan CL, Yew SM, Toh YF, Khoo J-S, Chong J, Lee KW, Tan Y-C, Yee W-
531 Y, Ngeow YF, Ng KP. 2015. Genome Analysis of the First Extensively Drug-Resistant
532 (XDR) Mycobacterium tuberculosis in Malaysia Provides Insights into the Genetic
533 Basis of Its Biology and Drug Resistance. PLoS One 10.

bioRxiv preprint doi: https://doi.org/10.1101/2020.12.01.407569; this version posted December 2, 2020. The copyright holder for this preprint (which was not certified by peer review) is the author/funder, who has granted bioRxiv a license to display the preprint in perpetuity. It is made available under aCC-BY-NC 4.0 International license.

534 47. Freidlin PJ, Nissan I, Luria A, Goldblatt D, Schaffer L, Kaidar-Shwartz H, Chemtob D,
535 Dveyrin Z, Head SR, Rorman E. 2017. Structure and variation of CRISPR and CRISPR-
536 flanking regions in deleted-direct repeat region Mycobacterium tuberculosis complex
537 strains. BMC Genomics 18:168.

538

539

540

541

542

bioRxiv preprint doi: https://doi.org/10.1101/2020.12.01.407569; this version posted December 2, 2020. The copyright holder for this preprint (which was not certified by peer review) is the author/funder, who has granted bioRxiv a license to display the preprint in perpetuity. It is made available under aCC-BY-NC 4.0 International license.

Table 1. Estimation of hard-core, soft-core and accessory sequence elements of 121 MTB genomes.

	Shared amongst 100% of the genome		**Shared among ≤90% of genome**	
Core genome characteristics	**Core genome Average (range)**	**Accessory genome Average (range)**	**Core genome Average (range)**	**Accessory genome Average (range)**
Size (bp)	3683161 (3672229-3751588)	696320.9 (461308-742152)	4308602 (4213348-44055935)	93819.7 (32024-135709)
GC content	65.1	67.9	65.5	71.7
Number of sequence segments	939 (894-1053)	936.3 (847-1116)	115 (112-658)	121.8 (47-219)
Maximum segment length	27136 (26906-33160)	3059.4 (15015-27765)	211154 (57005-377999)	7391.4 (290.2-15599)
Avg. segment length	3922.4 (3562.7-4170.6)	745.6 (544.6-8224.4)	37466.1 (6320-38375)	778.4 (331.4-1026.7)
Median length	2558 (2231-2746)	220.2 (179-253)	18237 (2599-20222)	289.6 (71-4400)
No. of CDS	3698 (3438-4173)	539.3 (443-629)	4237 (3887-4718)	57.6 (20-88)

[a]Core genome present in 100% of genomes

[b]Core genome present in ≤90% of geno

Table 2. Showing Sequence elements of CRISPR-associated endo-ribonuclease cas2 (*Rv2816c*); CRISPR-associated endonuclease cas1 (*Rv2817c*); CRISPR type III-a/mtube-associated protein csm6(*Rv2818c*); CRISPR type III-a/mtube-associated protein csm5 (*Rv2819c*) and CRISPR type III-a/mtube-associated ramp protein csm4 (*Rv2820*c) deleted among modern Beijing lineage taken in assortment for pangenome analysis.

Gene name	**Nucleotide sequences deleted in modern beijing lineage**
Rv2817c (Complete deletion)	atggtgcagctgtatgtctcggactccgtgtcgcggatcagctttgccgacggccgggtgatcgtgtggagcgaggagctcggcgagagccagtatccgatcgagacgctggacg gcatcacgctgtttgggcggccgacgatgacaacgcccttcatcgttgagatgctcaagcgtgagcgcgacatccagctcttcacgaccgacggccactaccagggccggatctca acacccgacgtgtcatacgcgccgcggctccgtcagcaagttcaccgcaccgacgatcctgcgttctgcctgtcgttaagcaagcggatcgtgtcgaggaagatcctgaatcagca ggccttgattcgggcacacacgtcggggcaagacgttgctgagagcatccgcacgatgaagcactcgctggcctgggtcgatcgatcgggctccctggcggagttgaacgggttc gagggaaatgccgcaaaggcatacttcaccgcgctggggcatctcgtcccgcaggagttcgcattccagggccgctcgactcggccgccgttggacgccttcaactcgatggtca gcctcggctattcgctgctgtacaagaacatcataggggcgatcgagcgtcacagcctgaacgcgtatatcggtttcctacaccaggattcacgagggcacgcaacgttggcgagc gacctcatggaggtatggcgggcgccgatcatcgatgacaccgtacttcgattgatcgcggacggtgtggtcgacacccgggctttcagcaagaactccgacacgggggccgtctt cgcgacacgggaagccacacgatccatcgcgcgcgcctttggtaatcgaatcgcacgaaccgccacctacatcaaaggcgatcctcaccgatacacctttcagtacgccctcgact tgcaactgcaaagcctcgtgcgtgttatcgaagccgggcacccgtcgcggctcgtcgatatcgatatcacctccgagccatccggagcctaa
Rv2816c (complete deletion)	Atgcccactcgcagccgtgaggagtacttcaatctcccgctcaaagtggacgagtccagcggcactataggcaagatgttcgtcctcgtaatatacgacatcagcgacaaccggcg gcgggcttcacttgcgaagatcctggccgggtttggctatcgcgtccaagagtccgcattcgaagcgatgctgacgaagggccagctcgcgaaactagttgcacgtatcgaccgctt cgccatcgactgcgacaacatccggatctataagataagaggtgttgcggcagttacgttctacggaaggggacggcttgtcagcgcagaggagtttgtgttcttttga
Rv2818c (complete deletion)	Gtgctattcctcagcgccgagatagctgcctttgagaacgcggaccggcggtactccgcggcaatcacgcggctcgcgcctgagaccgacgttcgcatagtcacctataccaacc cgtcggtgcacaggttcgacctttcgtgccggttttccgcaaccacctggttgaactgtcggctgagttccctgatcgaaccattctgctgaataccagttccggcacccctgcgatgc aggcggcgctggtggccataaatgtgtttggcattcccaggaccaccgctgtgcaagtaagcacgcctgcccgggcattgagcaagcctggcgatcgtgaatccccagacgcttac gacctcgaactaatgtgggacgcaaacgacgacaatcagcctggagcccccaaccgttgctttgaggcgacttccgctgcgctcggcgcgctgcttgagcgggccaacctgaagc agctgatcgtgtcgtacgactactcggcagcagtgacgatcgcggcagactcgcgcctgcccgatcaagtgagcaatctgatccgcggcgcgatgcaccgctcgaggctggaaca cctcgtagcgccaaagttctttaaggacaccgcgttcacgtatgaccccgcgaacaaggtcgctgagtacataagtgctcttgcgctgctggcaaagcgcgagcaatgggctgaatt cgcacgatcagctaccccggcaatcactatcgtgctcagggcggctgtggcaaaacaccttccggaggaccgctatctcgacgacatgggccgcgtcgaccgccgaaagctgga aagagagccggagatacggtgcgcgctcaagcaccctccgaaatcgccaaacgcggagtggtacctctacaccaaggactggctcgcactgctccgccaattcgcacccgatcg agttggtgctcttgaagtactcggaaggttcgagagccgggtccgcaacaccgcagcacacgagatcgtctcaatcagtgaggatcgcatcacgaaggatggcggccttctcccag aacaactgctgaagatcctcgcccgcgaaacaggcgctgatttgacgctctatgaccggttgaacgacgagatcatccggcagattgatatggcaccgctgggctaa

Rv2819 (complete deletion)	Atgaacacctacctgaagccgttcgaactcacgctgcggtgcctggggccggtgtttatcggatccggcgagaagcggacctcgaaggagtaccacgtggagggcgaccgggt ctacttcccggacatggaacttctttacgcagacattccggctcacaagaggaagtctttcgaagcgttcgtcatgaacaccgatggggcacaggcgacggcgccactcaaagagtg ggtagagccaaacgcggtcaagctggatcctgctaagcatcgaggttacgaggtgaagatcgggtcgatcgaaccgcgacgtgcatctcgtggtcgaggcgggcgcatgactcg aaagaagcttacgctcaacgagattcacgctttcatcaaagaccctcttggaaggccctacgtgccgggttcgactgtcaagggaatgcttcgcagcatctacctgcagtcgcttgtgc ataagcggacggcccaacctgttcgtgttccgggacaccagacgcgggagcaccggcagtacggcgaaaggtttgagcggaaggagttgcgcaaatcggggcgccccaacac ccgtccgcaagacgcggtcaacgacctgtttcaggcgatcagggtcaccgactcacctgcactgagaacaagcgatctgctgatctgccagaagatggacatgaatgtccacggca agcctgatggcctgccgctcttccgggaatgtttggcgccgggaacctcaatctcgcaccgcgtggtggtcgacaccagtcccaccgctcgcggcggctggcgtgagggcgagc ggttccttgaaacgctggccgagacagccgcgtccgtgaatcaggcgcgttacgcggagtacagagccatgtaccctggcgtgaacgcgatagttggcccaattgtctatctgggc ggcggagccggctatcggagcaagacctttgtcaccgaccaagacgacatggcgaaggtgctcgacgcccagttcgggaaggtagtcaagcacgtcgacaagacgcgcgaact acgcgtctcaccacttgtcttgaagcgaaccaagatcgacaacatatgctacgagatgggtcagtgcgagctgtcgatcaggagagccgaatga
Rv2820 (partial deletion 355-901bp)	atgaactcgcggctgtttaggttcgacttcgaccgcacacacttcggcgaccacggcctcgagtcgtccacgattagctgccccgcggacaccctctactctgcgctttgcgttgaag cgctacggatgggtggccagcagctgcttggcgaactcgttgcgtgctcgacgctgcggttgaccgatctgctgccctatgtggggcccgattacctggttcccaagcccctgcaca gcgttcggtccgacggctcaagtatgcagaagaagctggcgaagaagatcggctttcttcccgctgcccagcttggcagcttcctcgatggcacggccgacctgaaagaactcgcg gcgcggcagaccaagatcggtgtccacgccgtgtcagcgaaggcagcgatccacaacggaaagaaagacgccgacccgtaccgtgtcggctacttccggttcgagctggacgc gggtctgtggttgctggcgaccggatccgagtccgagctcggcctactcaccaggctgttgaaagggatctccgcg ctgggcggcgaacggacaagcgggttcggagcgtttaaccttaccgagtcagaagcacccgccgcactcacgccgacagtcgacgcggcc agtctgatgacgctcacgacatccctacccacggacgacgagctcgaagccgcactcgccggcgcgacgtaccgcctcgtcaagcgcagtggattcgtcgcgtcgagcacatac gctgacatgcccctgcgcaaacgcgacatctacaaa]ttcgccgccggctcggtcttctcgcgaccc ttccaaggaggcatcctcgacgtcagcctgggcggaaaccatccggtctacagctacgcgcgaccgctatttctcgcactcccggagtccgccgcatga

*The portion of the gene that is present in bin32_se00001(clustAge software generates small bins of accessory sequences please refer software for detailed information (23) is from nucleotide bases 351 through 909 which was found to be deleted in Beijing lineage.

Table 3. List of primers designed against CRISPR genomic elements using Primer 3 software

Gene region	Primer	Length	Tm	Sequence size	GC%	Sequence	Product size (bp)
CRISPR-associated endonuclease cas2	Left Primer	20	60.76	342	55	GCGGCACTATAGGCAAGATG	229
	Right Primer	20	59.76		50	ACTGCCGCAACACCTCTTAT	
CRISPR-associated endonuclease cas1	Left Primer	19	59.57	1017	57.89	GCTCCGTCAGCAAGTTCAC	494
	Right Primer	21	60.01		47.62	CGATCAATCGAAGTACGGTGT	
CRISPR type III-a/mtube-associated protein csm6	Left Primer	20	60.79	1149	50	GCTGGTGGCCATAAATGTGT	812
	Right Primer	20	59.55		50	TCAGCAGTTGTTCTGGGAGA	
CRISPR type III-a/mtube-associated ramp protein csm5	Left Primer	20	59.41	1128	55	CTACTTCCCGGACATGGAAC	848
	Right Primer	20	60.55		55	GGTCGGTGACAAAGGTCTTG	
CRISPR type III-a/mtube-associated ramp protein csm4	Left Primer	19	59.75	909	57.89	GGCCGACCTGAAAGAACTC	483
	Right Primer	18	60.35		61.11	AAGGGTCGCGAGAAGACC	

bioRxiv preprint doi: https://doi.org/10.1101/2020.12.01.407569; this version posted December 2, 2020. The copyright holder for this preprint (which was not certified by peer review) is the author/funder, who has granted bioRxiv a license to display the preprint in perpetuity. It is made available under aCC-BY-NC 4.0 International license.

Table 4. Spoligotype patterns of clinical isolates (50 Beijing and 50 Non-Beijing) used for evaluation of CRISPR sequences.

SIT	SPOLIGOTYPE DESCRIPTION	OCTAL CODE	LINEAGE	Total
1	□□□□□□□□□□□□□□□□□□□□□□□□□□□□□□□□■■■■■■■■■■	000000000003771	BEIJING	41
11	■□□■■■■■■■■■■■■■■■■■■■■■■■□□□□■□■■□□□■■■■■	477777777413071	EAI3 IND	5
26	■■■□□□□■■■■■■■■■■■■■■□□□□□□□□□□□□■■■■■■■■■■	703777740003771	CAS1 DELHI	4
34	■■■■■■■■□□■■■■■■■■■■■■■■■■■■■■■■□□□□■■■■■■	776377777760771	S	2
37	■■■■■■■■■■■■□■■■■■■■■■■■■■■■■■■■■□□□□■■■■■■■	777737777760771	T3	1
52	■■■■■■■■■■■■■■■■■■■■■■■■■■■■■■■■■■■■□□□□■■■□■■■	777777777760731	T2	1
53	■■■■■■■■■■■■■■■■■■■■■■■■■■■■■■■■■■■■□□□□■■■■■■■	777777777760771	T1	1
54	■■■■■■■■■■■■■■■■■■■■■■■■■■■■■■■■■■■■□□■■■■■■■■■	777777777763771	MANU2	3
67	■■■■■■■■■■■■□■■■■■□□□□■■■■■■■■■□■□□□□■■■■■■■	777777037720771	H3	2
119	■■■■■■■■■■■■■■■■□■■■■■■■■■■■■■■■■□□□□■■■■■■■	777776777760771	X1	4
127	■□■■■■■■■■■■■■■■■■■■■■■■■■■■■■■■□□□■□□□□■■■■■■■	577777777420771	H4	3
137	■■■■■■■■■■■■■■■■■□■■■■■■■■■■■■■■■□□□□■■□□□□■	777776777760601	X2	4
190	□□□□□□□□□□□□□□□□□□□□□□□□□□□□□□□□□□□□■■■■■□■■■	000000000003731	BEIJING	5
243	■■■■■■■■■■■■■■■■■■■■■■■■■■■■■■■■■■■■□□□□■■□□□□□	777777777760600	T1	3
283	■■■■■■■■■■■■■■■■■■■■■□□□■□□□□□□■□□□□■■■■■■■	777777704020771	H1	1
288	■■■□□□□□□□■■■■■■■■■■■■□□□□□□□□□□□□□■■■■■■■■■	700377740003771	CAS2	1
357	■■■□□□□■■■■■■■■■■■■■■■□□□□□□□□□□□□□□■■■■■■■■	703777740000771	CAS	2
428	■■■□□□□■■■■■■■■■■■■■■■□□□□□□□□□□□□□■■□■■■■■■	703777740003371	CAS1 DELHI	1
464	■■■■■■■■■■■■■■■■■■■■■■■■■■■■■■■■■■■■■□■■■■■■■■■	777777777747771	URAL	2
621	□□□□□□□□□□□□□□□□□□□□□□□□□□□□□□□□□□□□■□■■■■■■■	000000000002771	BEIJING	4
794	■■■□□□□■■■■■■□■■■■■■■■□□□□□□□□□□□□□■■■■■■■■■	703757740003771	CAS1 DELHI	2
1091	■■■□□□□■■■■■■■■■■■■■■■□□□□□□□□□□□□□■□■■■■■■■	703777740002771	CAS1 DELHI	1
1628	□□□■■■■■■■■■□■■■■■■■■■■■■■■■□□□□■□■■■■■■■■■■	077737777413771	EAI5	4
1970	■■■■■■■■■■■■■■■■■□■■■■■□■■■■■□□□□■□■■■■■■■■■■	777776757413771	EAI6 BGD	1
ORPHAN	■■■□□□□□□□□□□□□□□□□□□□□□□□□□□□□□□□□□■■■■■■■	700000000000771	CAS	2

bioRxiv preprint doi: https://doi.org/10.1101/2020.12.01.407569; this version posted December 2, 2020. The copyright holder for this preprint (which was not certified by peer review) is the author/funder, who has granted bioRxiv a license to display the preprint in perpetuity. It is made available under aCC-BY-NC 4.0 International license.

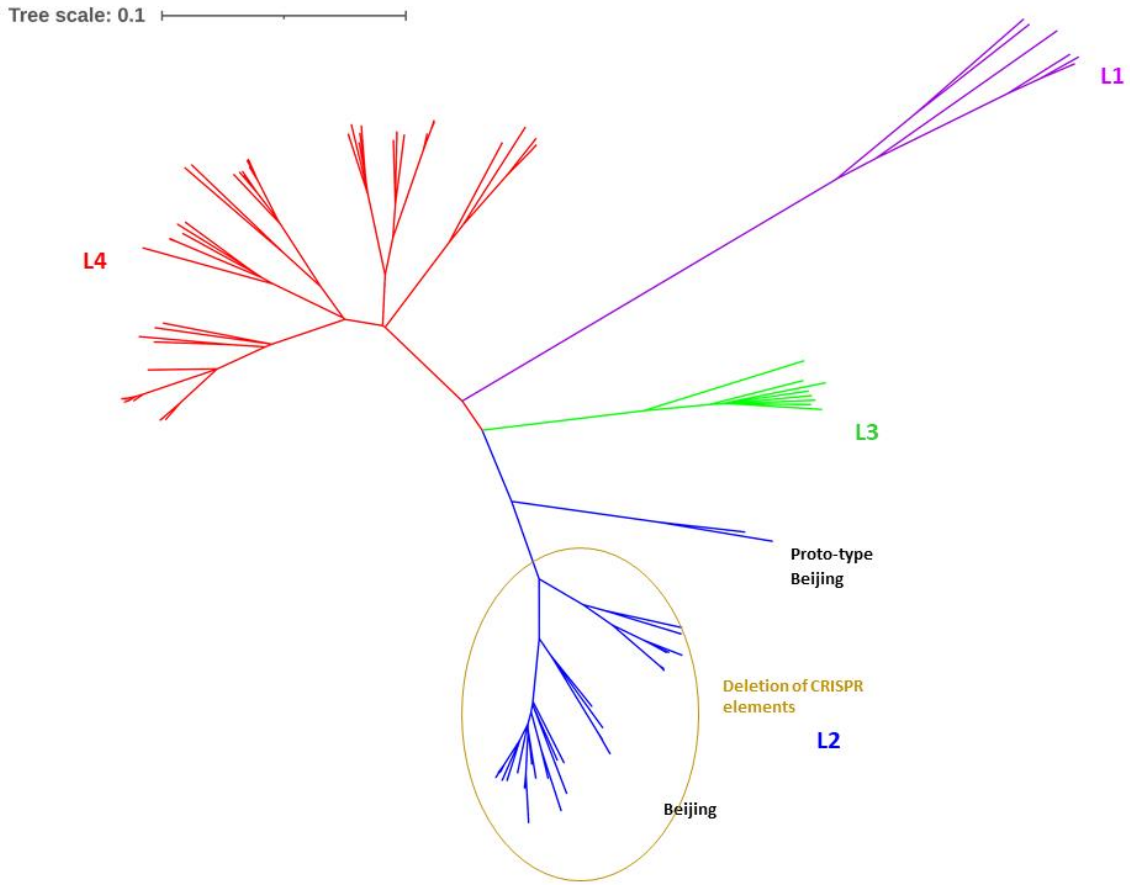

Fig. 1 Evolutionary parsimony tree was constructed by extended Majority Rule consensus using KSNP3.0. The tree shows four distinct lineages among 121 MTB isolates. Briefly, Purple lines represent clades belonging to Lineage 1 (Indian Oceanic); Blue lines represent clades belonging to Lineage 2 [East Asian (Beijing 40; proto-type Beijing 2)]; Green lines represent clade belonging to Lineage 3 (Central Asian); Red lines represent Lineage 4 (Euro-American).

bioRxiv preprint doi: https://doi.org/10.1101/2020.12.01.407569; this version posted December 2, 2020. The copyright holder for this preprint (which was not certified by peer review) is the author/funder, who has granted bioRxiv a license to display the preprint in perpetuity. It is made available under aCC-BY-NC 4.0 International license.

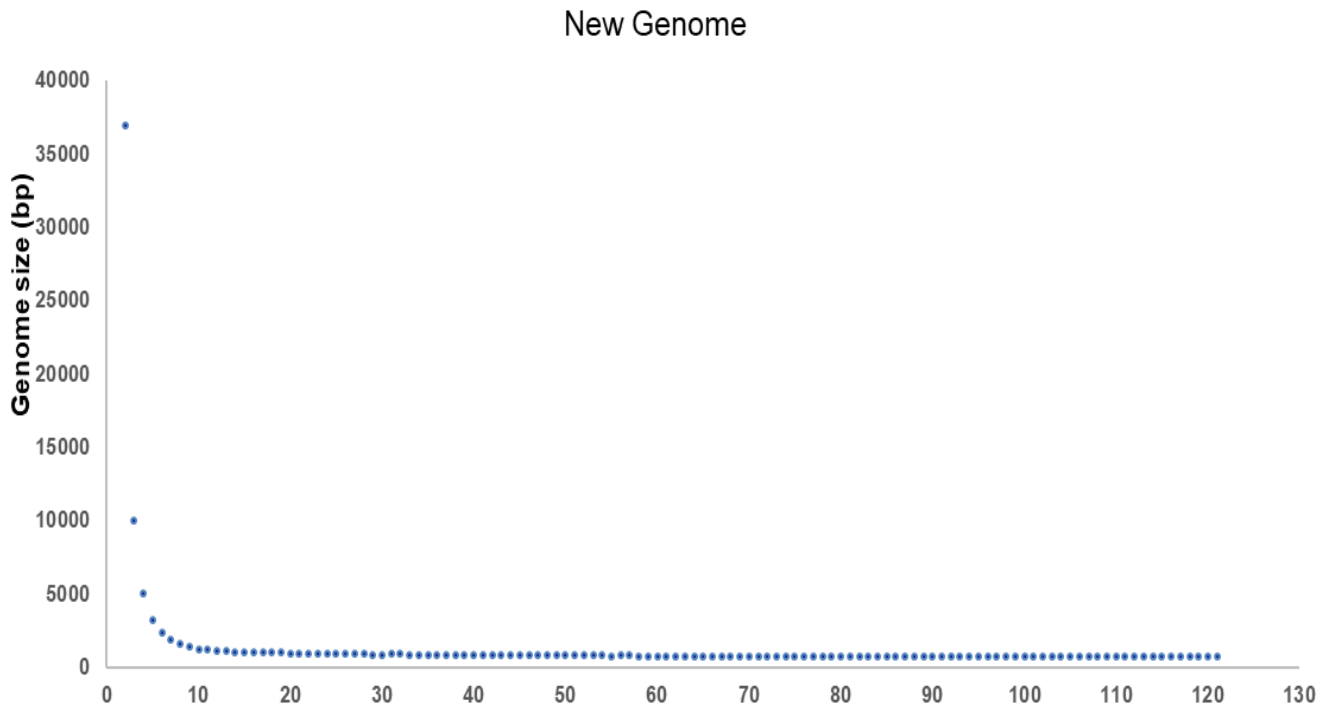

Fig 2. Representation of Core-Pan plot. Each marker represents the average core genome and pan-genome size of all possible permutations of genome orders for one hundred twenty for 10,000 randomly generated permutations adapted from *Tettelin et al., 2005* generated from Spine software.

bioRxiv preprint doi: https://doi.org/10.1101/2020.12.01.407569; this version posted December 2, 2020. The copyright holder for this preprint (which was not certified by peer review) is the author/funder, who has granted bioRxiv a license to display the preprint in perpetuity. It is made available under aCC-BY-NC 4.0 International license.

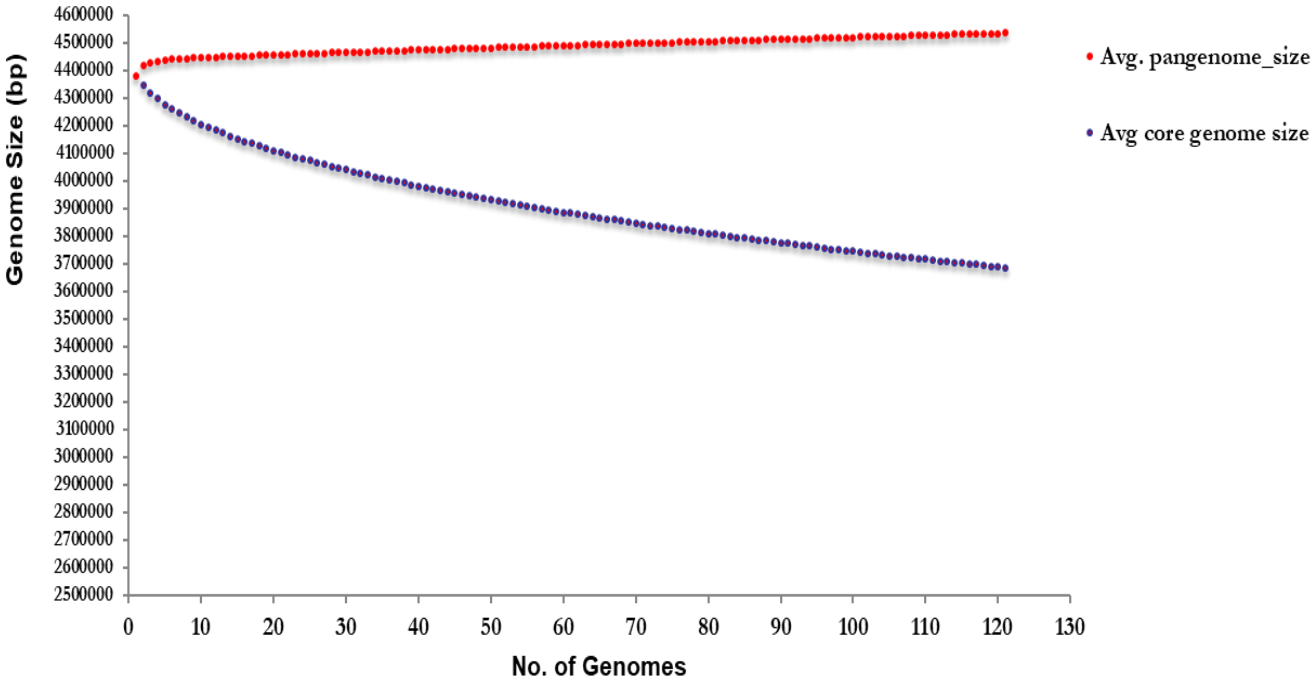

Fig. 3. New genome size of genome orders for one hundred twenty-one for 10,000 randomly generated permutations.

bioRxiv preprint doi: https://doi.org/10.1101/2020.12.01.407569; this version posted December 2, 2020. The copyright holder for this preprint (which was not certified by peer review) is the author/funder, who has granted bioRxiv a license to display the preprint in perpetuity. It is made available under aCC-BY-NC 4.0 International license.

Fig. 4A

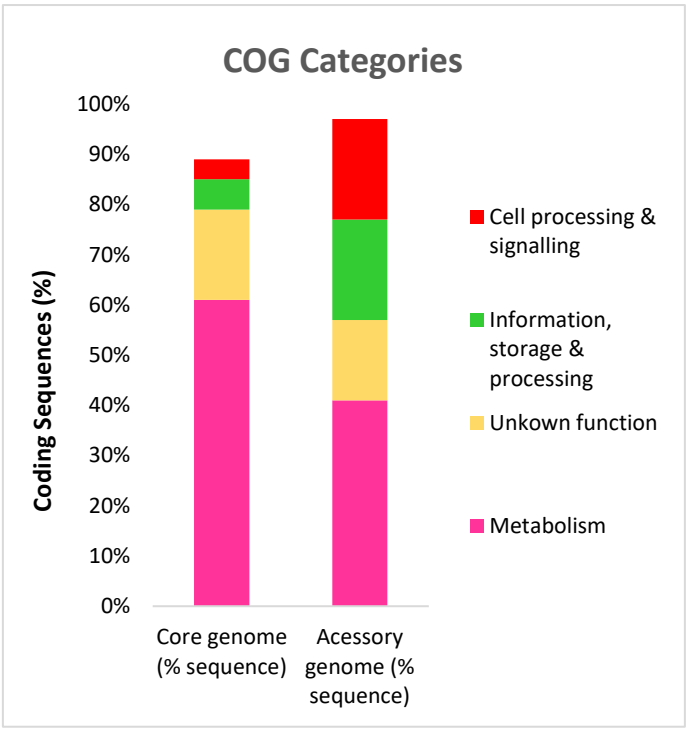

Fig. 4B

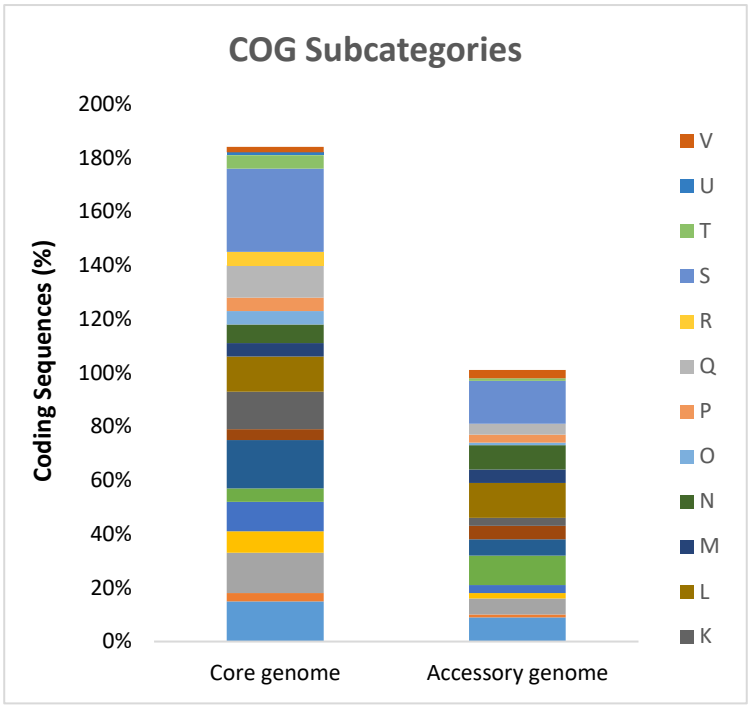

Fig.4a Functional annotations of core and accessory genes (A) COG categories **Fig. 4b**(B) COG subcategories of predicted genes within the core and accessory genomes of *M. tuberculosis* genomes by eggNOG Mapper v2.0. Each category or subcategory is graphed as a percentage of the total number of genes in the core or accessory genomes.

Sub-categories abbreviations include;

1. Cellular processes and signaling {[D] Cell cycle control, cell division, chromosome partitioning, [M] Cell wall/membrane/envelope biogenesis, [N] Cell motility, [O] Post-translational modification, protein turnover, and chaperones, [T] Signal transduction mechanisms, [U] Intracellular trafficking, secretion, and vesicular transport [V] Defense mechanisms [W] Extracellular structures [Y] Nuclear structure [Z] Cytoskeleton} 2.Information storage & processing {[A] RNA processing and modification [B] Chromatin structure and dynamics [J] Translation, ribosomal structure and biogenesis [K] Transcription [L] Replication, recombination and repair} 3.Metabolism {[C] Energy production and conversion [E] Amino acid transport and metabolism [F] Nucleotide transport and metabolism [G] Carbohydrate transport and metabolism [H] Coenzyme transport and metabolism [I] Lipid transport and metabolism [P] Inorganic ion transport and metabolism [Q] Secondary metabolites biosynthesis, transport, and catabolism} poorly characterized [R] General function prediction only [S] Function unknown

bioRxiv preprint doi: https://doi.org/10.1101/2020.12.01.407569; this version posted December 2, 2020. The copyright holder for this preprint (which was not certified by peer review) is the author/funder, who has granted bioRxiv a license to display the preprint in perpetuity. It is made available under aCC-BY-NC 4.0 International license.

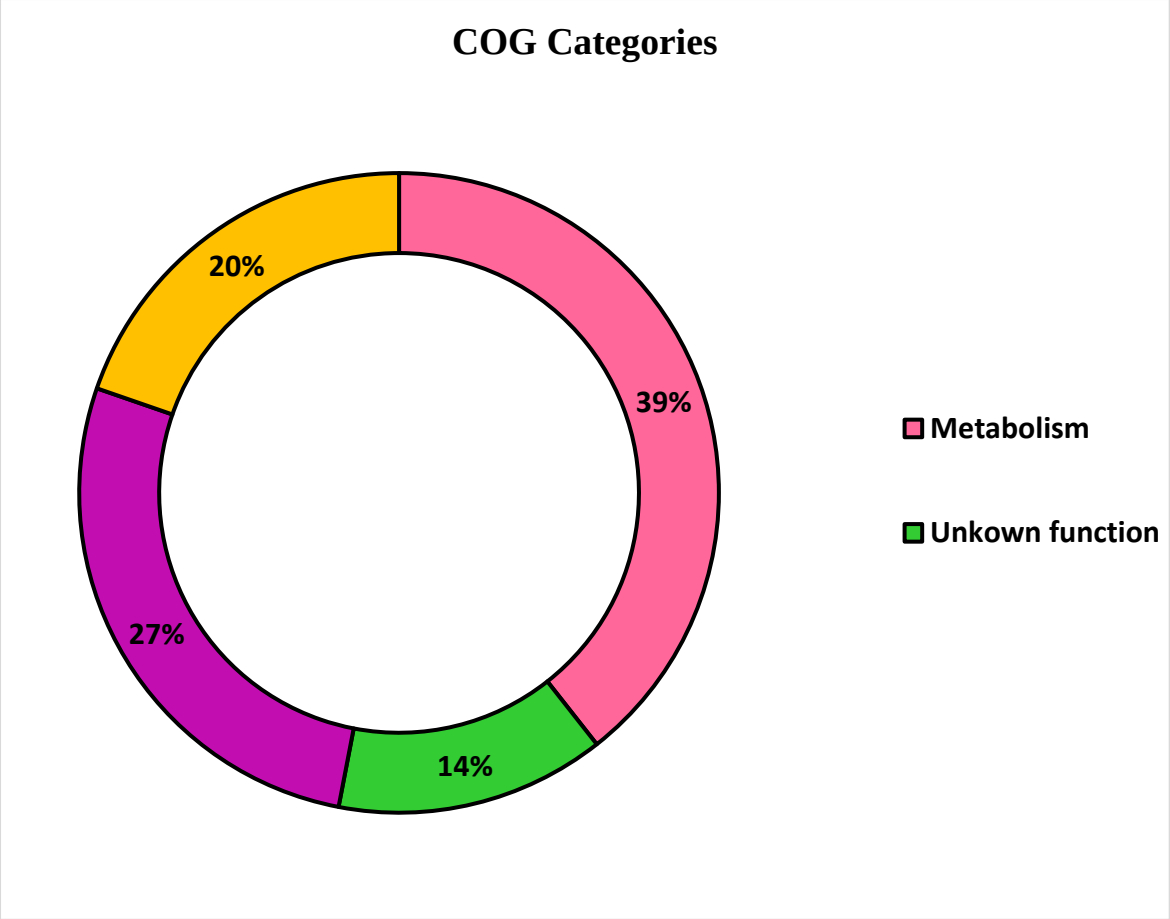

Fig 5. Functional annotations of unique gene COG categories of *M. tuberculosis* genomes by eggNOG Mapper v2.0.

bioRxiv preprint doi: https://doi.org/10.1101/2020.12.01.407569; this version posted December 2, 2020. The copyright holder for this preprint (which was not certified by peer review) is the author/funder, who has granted bioRxiv a license to display the preprint in perpetuity. It is made available under aCC-BY-NC 4.0 International license.

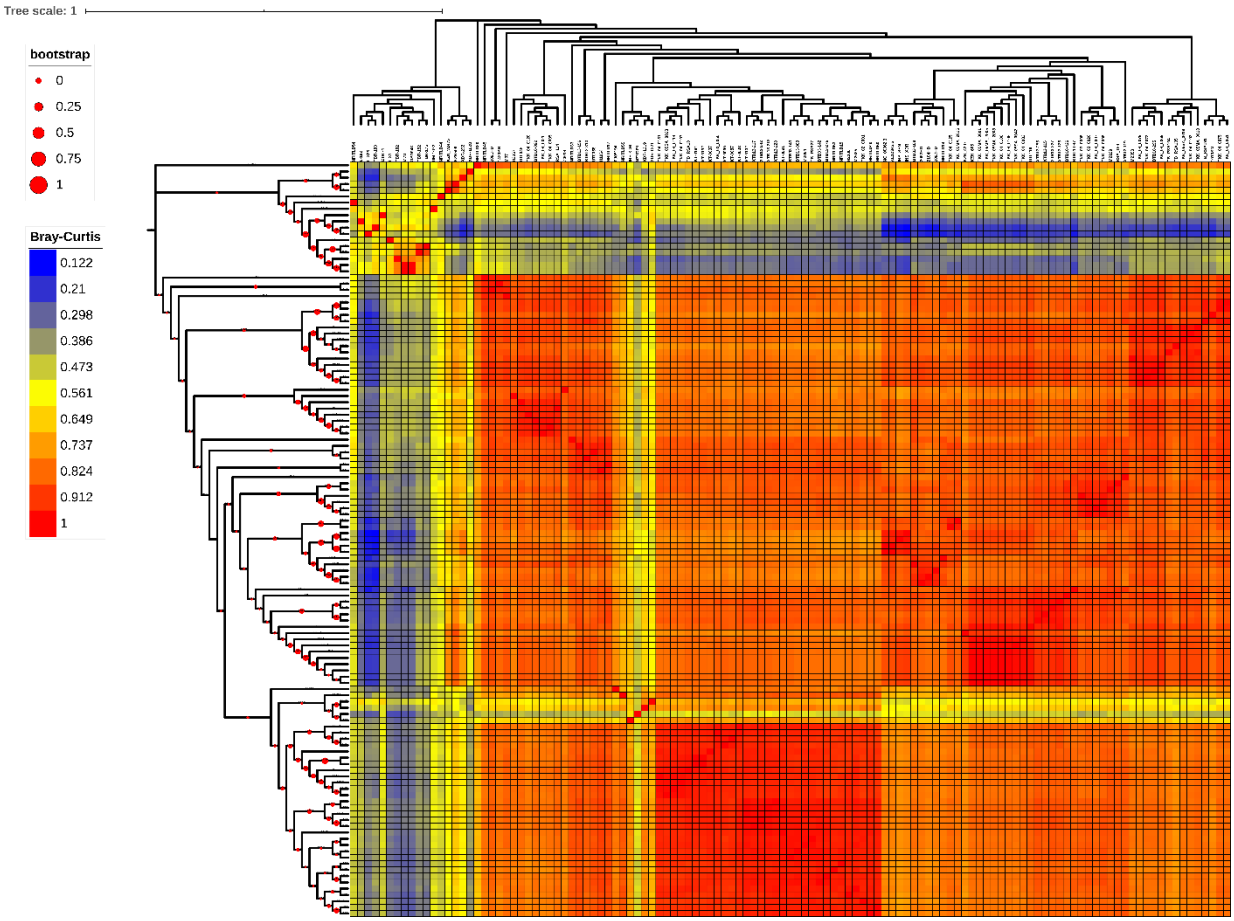

Fig.6 Neighbor joining tree and heat map generated by ClustAGE software showing distribution of accessory elements across 121 *M. tuberculosis* genomes.

Neighbor joining tree and heat map of accessory element distribution patterns was calculated using Bray-Curtis distance matrix by ClustAGE software from distributions of accessory elements. Tree and heat map files were viewed iTOL (https://itol.embl.de)

bioRxiv preprint doi: https://doi.org/10.1101/2020.12.01.407569; this version posted December 2, 2020. The copyright holder for this preprint (which was not certified by peer review) is the author/funder, who has granted bioRxiv a license to display the preprint in perpetuity. It is made available under aCC-BY-NC 4.0 International license.

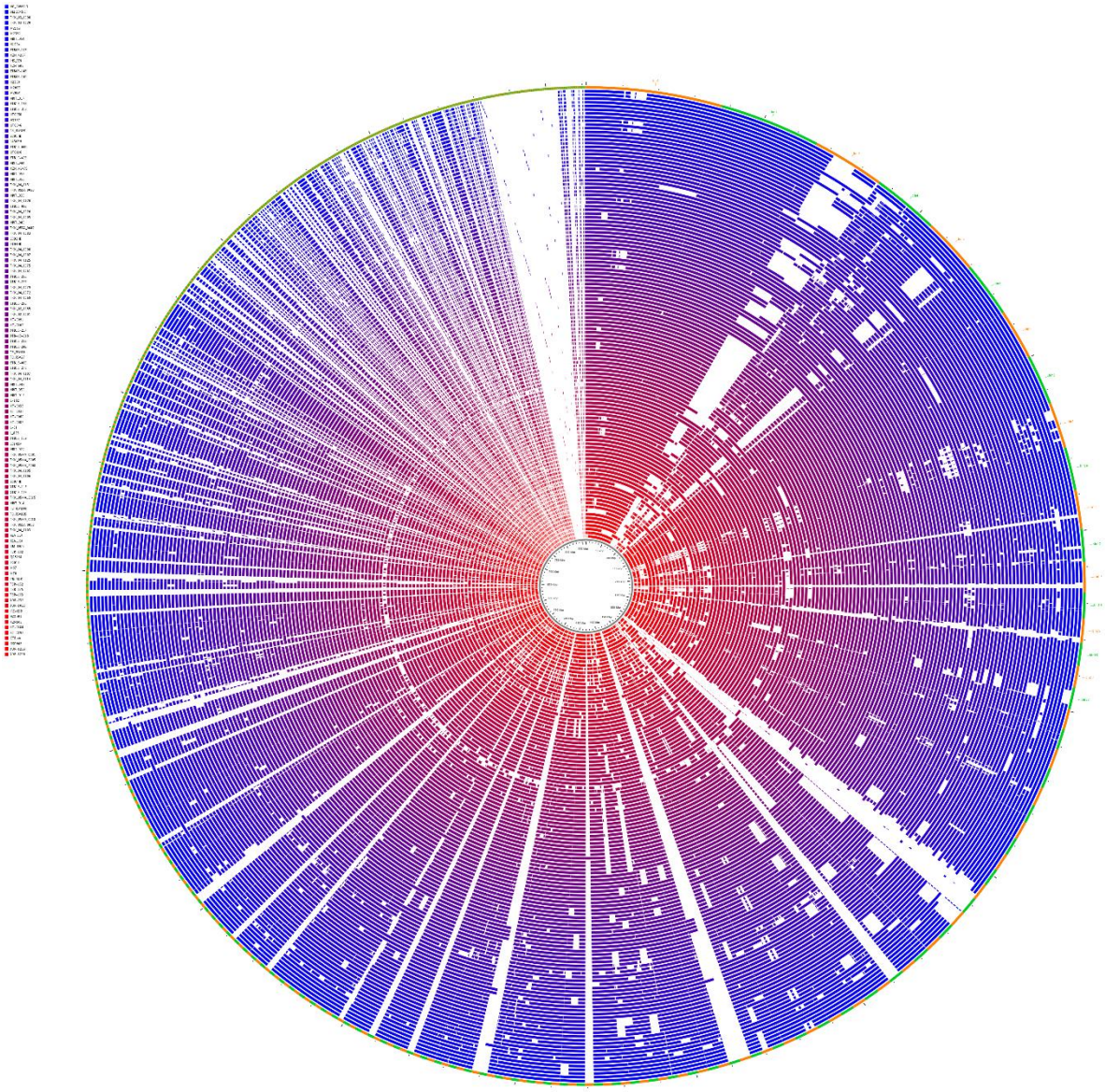

Fig. 7A. ClustAGE plot Sharing of accessory sequences present in all 121 MTB strains (100% core)

bioRxiv preprint doi: https://doi.org/10.1101/2020.12.01.407569; this version posted December 2, 2020. The copyright holder for this preprint (which was not certified by peer review) is the author/funder, who has granted bioRxiv a license to display the preprint in perpetuity. It is made available under aCC-BY-NC 4.0 International license.

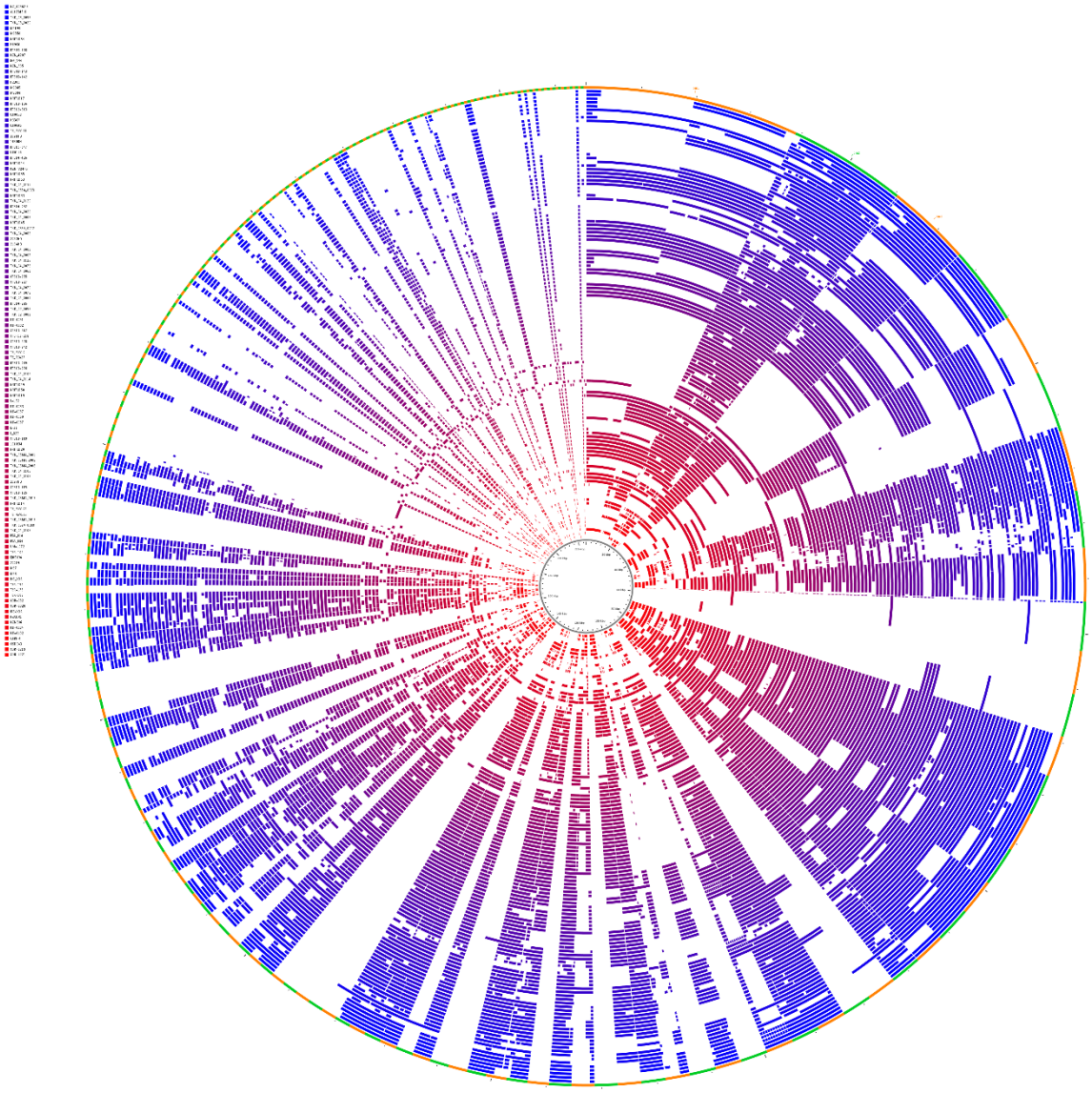

Fig. 7B. ClustAGE plot Sharing of accessory sequences of sequences or and in ≥ ≤110 MTB strains (90%)

bioRxiv preprint doi: https://doi.org/10.1101/2020.12.01.407569; this version posted December 2, 2020. The copyright holder for this preprint (which was not certified by peer review) is the author/funder, who has granted bioRxiv a license to display the preprint in perpetuity. It is made available under aCC-BY-NC 4.0 International license.

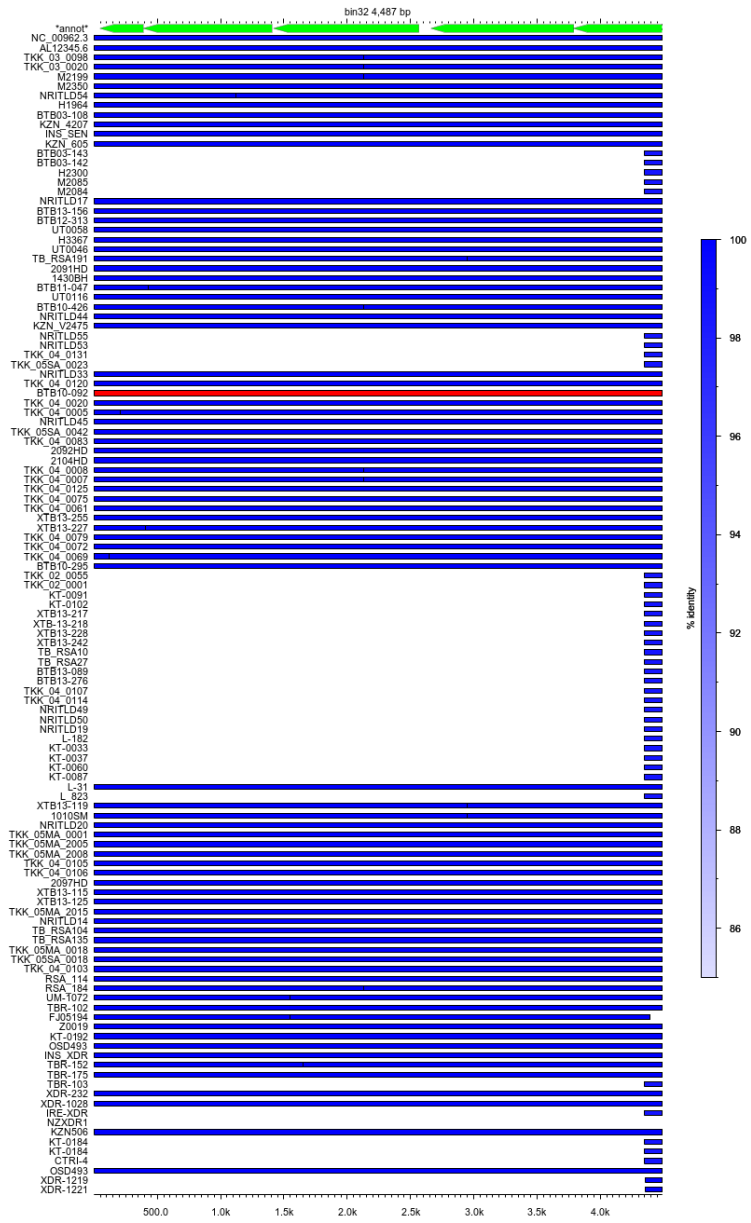

Fig 8. AGE graph output showing Bin 32; total size 4487 bp segment, completely deleted sequences in Beijing lineage are CRISPR-associated endo-ribonuclease cas2 (*Rv2816c*); CRISPR-associated endonuclease cas1 (*Rv2817c*); CRISPR type III-a/mtube-associated protein csm6 (*Rv2818c*); CRISPR type III-a/mtube-associated ramp protein csm5 (*Rv2819c*) and partially deleted CRISPR type III-a/mtube-associated ramp protein csm4 (61.5%) respectively

bioRxiv preprint doi: https://doi.org/10.1101/2020.12.01.407569; this version posted December 2, 2020. The copyright holder for this preprint (which was not certified by peer review) is the author/funder, who has granted bioRxiv a license to display the preprint in perpetuity. It is made available under aCC-BY-NC 4.0 International license.

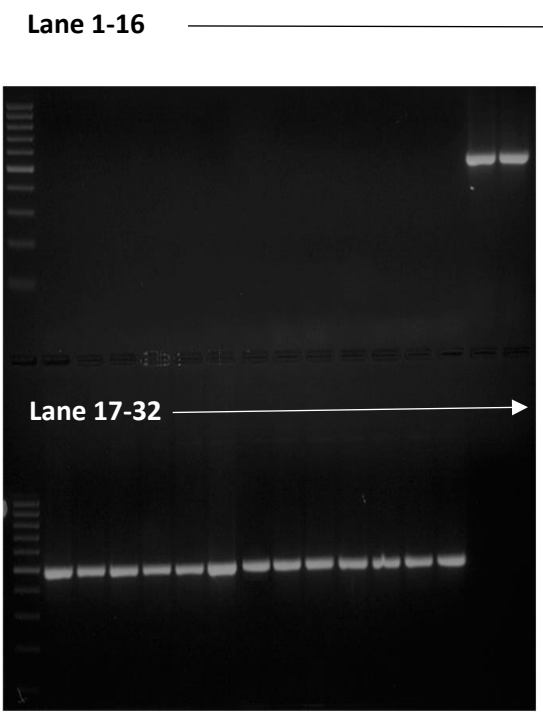

Lane 1 (1Kb DNA Ladder)

Lane 2-13 (Beijing Lineage)

Lane 14 (NC; Distilled Water

Lane 15-16 (PC; H37Rv)

Lane 17 (1Kb DNA Ladder)

Lane 18-29 (Non-Beijing Lineage)

Lane 30-31 (H37Rv)

Lane 32 (NC; Distilled Water)

Amplified Product: 229bp

Fig. 9A Representation pic showing CRISPR Cas2 (*Rv2816c*) sequence elements deleted in Beijing

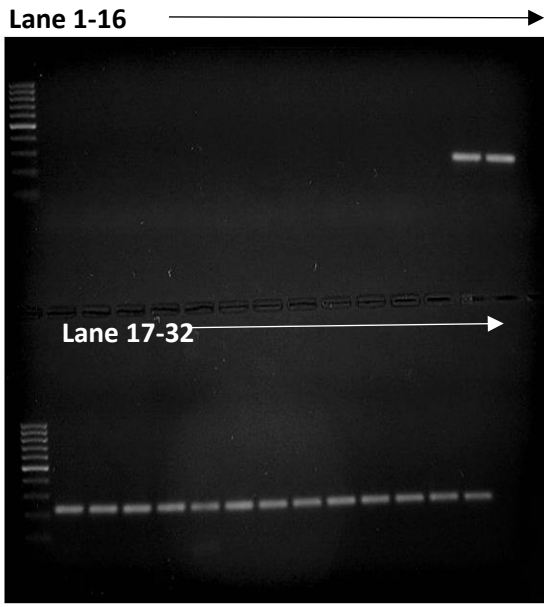

Lane 1 (1Kb DNA Ladder)

Lane 2-13 (Beijing Lineage)

Lane 14- (NC; Distilled Water

Lane 15-16 (H37Rv)

Lane 17 (1Kb DNA Ladder)

Lane 18-29 (Non-Beijing Lineage)

Lane 30-31 (H37Rv)

Lane 32 (NC; Distilled Water)

Amplified Product: 494bp

Fig.9B. Representation pic showing CRISPR Cas1 (*Rv2817c*) sequence elements deleted in Beijing